

# Accepted Manuscript

Low temperature synthesis and characterization of pure lanthanum hexaboride nanocrystals

Tuncay Simsek, Arun K. Chattopadhyay, Mustafa Baris, Murat Bilen



PII: S0022-4596(19)30216-6

DOI: <https://doi.org/10.1016/j.jssc.2019.04.039>

Reference: YJSSC 20740

To appear in: *Journal of Solid State Chemistry*

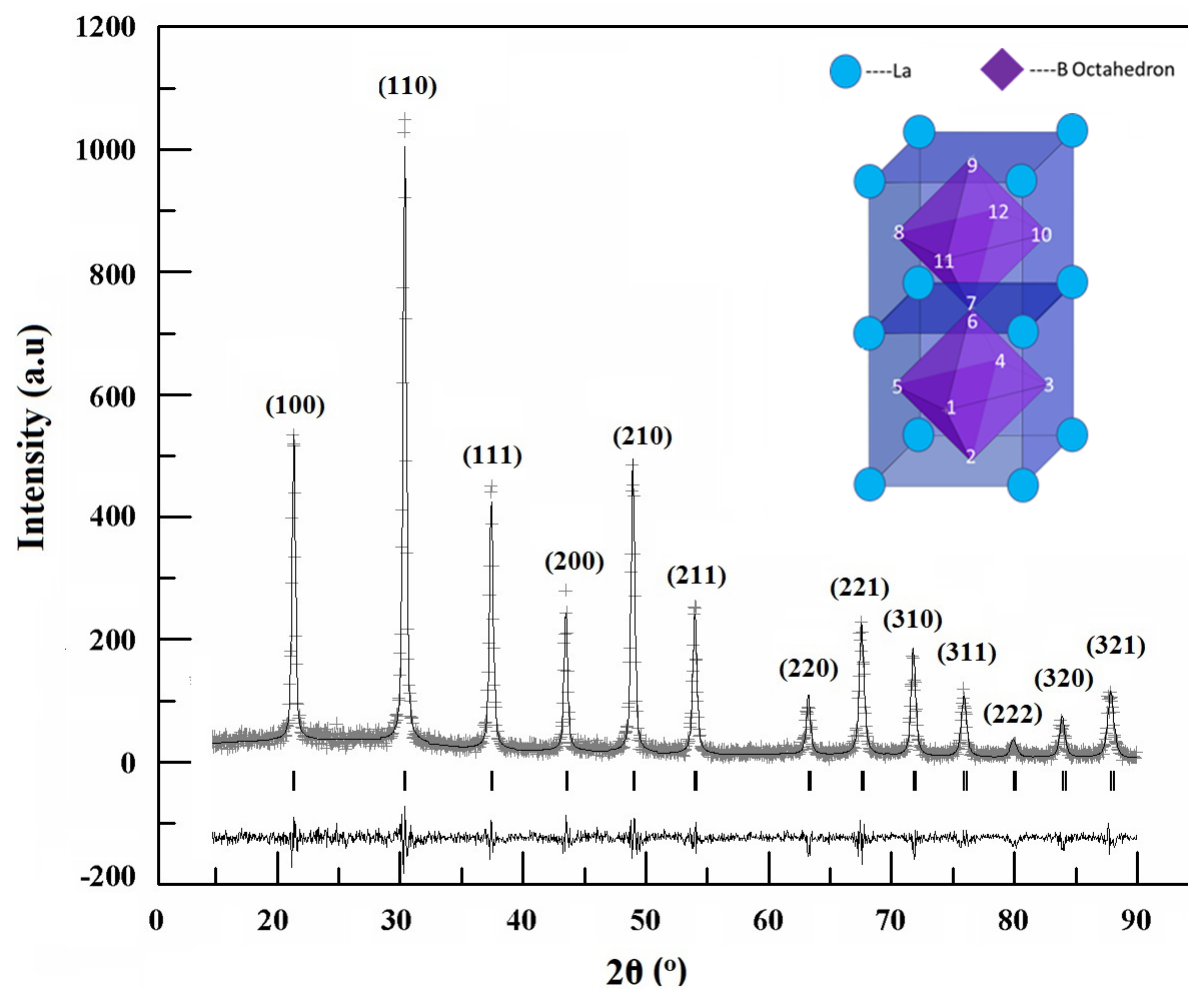
Received Date: 21 January 2019

Revised Date: 7 April 2019

Accepted Date: 28 April 2019

Please cite this article as: T. Simsek, A.K. Chattopadhyay, M. Baris, M. Bilen, Low temperature synthesis and characterization of pure lanthanum hexaboride nanocrystals, *Journal of Solid State Chemistry* (2019), doi: <https://doi.org/10.1016/j.jssc.2019.04.039>.

This is a PDF file of an unedited manuscript that has been accepted for publication. As a service to our customers we are providing this early version of the manuscript. The manuscript will undergo copyediting, typesetting, and review of the resulting proof before it is published in its final form. Please note that during the production process errors may be discovered which could affect the content, and all legal disclaimers that apply to the journal pertain.



# Low Temperature Synthesis and Characterization of Pure Lanthanum Hexaboride Nanocrystals

Tuncay Simsek<sup>1</sup>

<sup>1</sup>*Department of Industrial Design, Mersin University, Mersin 33343, Turkey*  
<sup>1</sup>[tuncaysimsek@mersin.edu.tr](mailto:tuncaysimsek@mersin.edu.tr),

Arun K. Chattopadhyay<sup>2</sup>

<sup>2</sup>*Uniformity Labs, 41400 Christy Street, Fremont, CA 94538*  
<sup>2</sup>[chattopadhyay@uniformitylabs.com](mailto:chattopadhyay@uniformitylabs.com)

Mustafa Baris<sup>3</sup>

<sup>3</sup>*Eti Maden Works General Management, 06010, Ankara, Turkey.*  
<sup>3</sup>[mustafabaris@etimaden.gov.tr](mailto:mustafabaris@etimaden.gov.tr),

Murat Bilen<sup>4</sup>

<sup>4</sup>*Eti Maden Works General Management, 06010, Ankara, Turkey.*  
<sup>4</sup>[mbilen@etimaden.gov.tr](mailto:mbilen@etimaden.gov.tr)

Corresponding author: Tuncay SIMSEK

Address: Department of Industrial Design, Mersin University, Mersin 33343, Turkey

Fax: +90 324 361 01 09

Tel: +90 324 361 00 01

E-mail: [tuncaysimsek@mersin.edu.tr](mailto:tuncaysimsek@mersin.edu.tr)

## Abstract:

This study aims to synthesize very pure form of LaB<sub>6</sub> nanocrystals at low temperatures. The synthetic route employed involved low temperature magnesiothermic reduction process of La<sub>2</sub>O<sub>3</sub> with a mixture of Mg, I<sub>2</sub> and B<sub>2</sub>O<sub>3</sub> at 90 °C. The powder mixtures were mechanically induced under Ar atmosphere for 3 hours and then heat treated. The pure form of nano LaB<sub>6</sub> powder produced by this technic is by far the most versatile route for the synthesis of nano-LaB<sub>6</sub>. From the XRD evidences of the synthesized powders, a correct reaction path for the reduction process has been elucidated. The average particle size of nano powder synthesized was estimated from SEM as well as XRD as 78±12 nm and 61.3±2.0 nm respectively, and the values were found to be in good agreement. The particle size determined by XRD was upon applying the Rietveld refinement method and using isotropic Lorentzian Scherrer particle broadening parameter (LX) of refined peak profiles. From the average size of the particulates and from the specific surface area of LaB<sub>6</sub> (1.3 m<sup>2</sup>/g) as determined by BET method, the number of unit crystals that might have constituted a nano-particulate of size 61.3±2.0 nm was estimated as 10<sup>5</sup> numbers from the crystallographic information of LaB<sub>6</sub>.

**Keywords:** Magnesiothermic method;  $\text{LaB}_6$ ; nanocrystals; leaching.

## 1. Introduction

Metal borides in general are of great importance as ceramic materials due to their high hardness, high heat and electrical conductivity, good abrasion, thermal shock and corrosion resistance properties, and for an excellent chemical stability at high temperatures [1-7]. Amongst all metal borides, rare-earth hexaborides ( $\text{RB}_6$ ; where  $\text{R}=\text{La}, \text{Ce}, \text{Pr}, \text{Nd}, \text{etc.}$ ) as refractory ceramics occupy a special place because of their low work function, which attributes to their high electron emissivity, super-conductivity, ferro-magnetism, narrowband semi-conductivity, etc. Lanthanum hexaboride ( $\text{LaB}_6$ ) in these respects is especially important for its highest electron emissivity hitherto known, and also for its excellent vacuum stability. One of the few major areas of usage of  $\text{LaB}_6$  is for its hot cathodic application either in a single crystal form or as coatings deposited by physical vapor deposition. Because of its low work function (2.6eV) and low vapor pressure at high temperatures,  $\text{LaB}_6$  has been considered as the material of choice for thin film coatings applications for both decorative and hard coatings [8]. Ceramics composites containing  $\text{LaB}_6$  are gaining more and more importance in application sciences particularly as support for transition metal catalysts [9]. Recent findings on nano- $\text{LaB}_6$  showed its high effectiveness to absorb near-infrared emissions, which opened the new field of potential applications in reducing solar heat gains [10]. The nano  $\text{LaB}_6$  powder is particularly considered as a material of great interest for coating filaments, carbon nano tubes and silicon field-emitters to lower work function in order to improve their electron-emissivity [11]

Various synthetic methods are commonly used for the synthesis of nano metal borides, such as borothermal [12], carbothermal [13], magnesiothermic reduction and electrochemical synthesis in molten salt [14-15], solvothermal [16], combustion sythnthesis (SHS) [17], mechanochemical [18] and floating zone method [19]. The synthesis of  $\text{LaB}_6$  via magnesiothermal method is particularly beneficial due to the fact that they can be formed at relatively low reaction temperatures. In this work, pure  $\text{LaB}_6$  nanocrystals were synthesized by magnesiothermic reaction using  $\text{La}_2\text{O}_3$ ,  $\text{B}_2\text{O}_3$ ,  $\text{I}_2$  and Mg powders at 90 °C. The effect of stoichiometry and temperature on the synthesized nano-phase of  $\text{LaB}_6$  were investigated in detail. Their microstructures and phase characteristics were studied by X-ray diffraction and electron microscopy. From the average size of the particulates ( $28.3 \pm 3.0$  nm) as determined

by Scherer formula and from the surface area ( $1.3 \text{ m}^2/\text{g}$ ) analysis, it was approximated that each particulate of the  $\text{LaB}_6$  nano-powder was comprised of approximately 600 unit-crystals of  $\text{LaB}_6$  in an average.

## 2. Experimental Method

### 2.1. Materials

As starting materials  $\text{La}_2\text{O}_3$  ( $< 100 \text{ nm}$ , 99.99%, Sigma Aldrich),  $\text{B}_2\text{O}_3$  ( $545.74 \text{ }\mu\text{m}$ ,  $>98.00\%$ , Eti Maden),  $\text{I}_2$  (99.7%, 1-3 mm, Sigma Aldrich) and Mg ( $138.66 \text{ }\mu\text{m}$ ,  $\geq 99.00\%$ , Sigma Aldrich) were used for the synthesis of  $\text{LaB}_6$ .  $\text{B}_2\text{O}_3$  was vacuum desiccated for more than 24 h prior to using in order to avoid any moisture ingress. All ball milling and magnesiothermic reduction processes were conducted under Argon gas (99.999%) atmosphere. 5 M Hydrochloric (HCl) acid solution was used for the purpose of leaching out MgO formed as a byproduct in order to produce pure form of nano-crystalline  $\text{LaB}_6$  from the reaction mix.

### 2.2. Magnesiothermic Reduction

The pre-weighed stoichiometric powder mixtures of  $\text{La}_2\text{O}_3$ , Mg,  $\text{B}_2\text{O}_3$  and  $\text{I}_2$  were placed in a grinding vial in a glovebox, and then the powder mixtures were milled under Argon atmosphere for 3 hours at 300 rpm in a ball mill (Fritch, P6) to prepare refined homogenous blends with reduced particle size. All samples must be handled very carefully under Argon atmosphere and devoid of any oxygen, in order to evade the possibility of any explosive reaction. The magnesiothermic reduction of the ball-milled powder mixture was conducted in a quartz tube. The quartz tube containing the reaction powder mixture was gradually heated to  $90 \text{ }^\circ\text{C}$  in an ash furnace maintaining a heating rate of  $2 \text{ }^\circ\text{C}/\text{min}$  under Ar atmosphere. The magnesiothermic reduction process followed almost instantaneously as soon as the temperature reached  $90 \text{ }^\circ\text{C}$  to form nano-particles of  $\text{LaB}_6$  and MgO,  $\text{Mg}_3(\text{BO}_3)_2$  and LaOI as byproducts. The product mixture obtained after the magnesiothermic reduction reaction was leached with 5M hydrochloric acid (HCl) acid solution at  $70 \text{ }^\circ\text{C}$  for 45 min with magnetic stirring at 400 rpm to remove all unwanted phases from the mixture. After the acid leaching process was complete, the slurry was centrifuged to separate  $\text{LaB}_6$  and then it was vacuum dried under 20 mbar pressure in a vacuum oven (Mettler VO-400) at  $80 \text{ }^\circ\text{C}$  for 12h forming pure nanocrystalline powders of  $\text{LaB}_6$ .

For the preparation of  $\text{LaB}_6$  nanocrystalline powders, four different starting powder mixture recipes were pursued to optimize the yield of  $\text{LaB}_6$ . The molar ratios of the mixtures of  $\text{La}_2\text{O}_3$ , Mg,  $\text{I}_2$ ,  $\text{B}_2\text{O}_3$  as shown in Table 1.

Table 1. Experimental conditions and the ratio of the powder mixtures used ( $\text{La}_2\text{O}_3$ :Mg: $\text{I}_2$ : $\text{B}_2\text{O}_3$ )

	A	B	C	D
Stoichiometry (mol)	1:44:6:12	1:48:6.6:13.3	1:58.5:8:16	1:88:12:24
Temperature ( $^{\circ}\text{C}$ )	90			
Period (min)	0-50			
Atmosphere	Argon			

### 2.3. Characterization of the powders

Malvern Mastersizer-2000 was used for the particle size analysis of all precursor powders used for the synthesis of  $\text{LaB}_6$ . The phase structure of the powders was determined by X-ray diffractometer (Rigaku D / MAX-2200) with  $\text{Cu K}\alpha$  radiation. A scanning rate of  $4^{\circ}$  per minute was used to scan over the range between  $2^{\circ}$  and  $90^{\circ}$  ( $2\theta$ ). Identification of crystalline phases were determined by the files of International Center for Diffraction Data (ICDD) powder diffraction. Morphology of the powders were determined by scanning electron microscopy (SEM) (FEI Quanta-200F) and the surface areas of the powders were determined by BET method (Quantaochrome Nova 220E). From the SEM of the nano-powders, particle sizes were determined by using the image processing program ImageJ Analyzer software [20]. The crystal structure as obtained by the XRD's of the purified powders was refined with Rietveld method using General Structure Analysis System (GSAS) [21]. The initial atomic coordinates of La and B in the  $\text{LaB}_6$  phase are given in Table 2 and full occupancy was assumed for La and B.

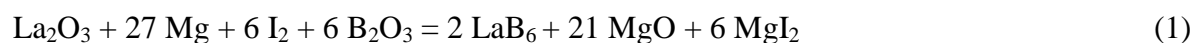
### 3. Results and Discussion

The average particle sizes ( $d_{50}$ ) for the starting powders of  $\text{La}_2\text{O}_3$  (*hexagonal*, ICDD Card No: 01-073-2141), Mg (*hexagonal*, ICDD Card No: 01-089-5003) and  $\text{B}_2\text{O}_3$  (*cubic*, ICDD Card

No: 06-0297) used were about 5.4  $\mu\text{m}$ , 137.6  $\mu\text{m}$  and 597.9  $\mu\text{m}$ , respectively. As starting materials not all of them had any similarity with respect to their sizes and size distributions. Iodine (*orthorhombic*, ICDD Card No: 00-043-0304) used for the synthesis was rather very large in size compared to other components of the powder mix. Nevertheless, the individual sizes of the ingredients were of limited significance as starting materials as they were all ball milled for their size refinement. The starting powder mixtures were refined in a high energy ball-mill for 3 hours for homogenization and reduction of their primary particle sizes. The employed ball-milling was quite aggressive maintaining a powder to ball charge weight ratio at 1:18 for comminution prior to carry out the magnesiothermic reaction.

For the purpose of optimizing the conditions of synthesis, four formulation samples of varying mixing ratios marked as A, B, C and D (Table1) were first homogenized and then subjected to heat treatment process to produce  $\text{LaB}_6$  [22]. All handling and milling processes were performed under Ar atmosphere. The homogenized powder mixture of the reactants first sealed into an argon-filled container, and then gradually heated to 90  $^\circ\text{C}$  at an incremental rate of 2 $^\circ\text{C}/\text{min}$ . At this temperature, the powder mixture reacted almost instantaneously forming  $\text{LaB}_6$  and other reaction byproducts. However, it is to recognize, at temperatures below the melting point of iodine, iodine sublimates until the equilibrium vapor pressure is reached, where several independent equilibria are effectively possible during the reduction process. As reported by others for similar type of magnesiothermic reductions [23, 24], in this co-reduction method of  $\text{La}_2\text{O}_3$  and anhydrous boric acid by Mg in the presence of  $\text{I}_2$ ,  $\text{I}_2$  actually enables the reaction to happen at lower temperatures than other magnesiothermic reduction process with iodine. Iodine in all probabilities acts as a catalyst that can greatly reduce the activation energy of reactions between  $\text{La}^{+++}$  and B. Following the dissociation equilibrium of iodine,  $\text{I}_2(\text{g}) \leftrightarrow 2\text{I}(\text{g})$ , both La and Mg can form metal iodides or other intermediates so the reaction can undergo at lower temperatures. Similar reactions without using iodine are not known to form hexaborides even at 650  $^\circ\text{C}$  [24].

Going by the conventional wisdom and as reported by other authors as well, the intuitive reaction path for the synthesis of  $\text{LaB}_6$  using magnesiothermic reduction process [24-26], should have been as expressed in Eq. 1.



However, the XRD pattern of the synthesized powders prior to leaching brought about the fact that the reaction was of very different nature in the presence of  $I_2$  than it was originally thought to be. The XRD's of the as-prepared powders as shown in Fig. 1 revealed that the reaction products were actually the mixtures of  $LaB_6$  (ICDD Card No:01-073-1669),  $Mg_3(BO_3)_2$  (ICDD Card No:01-073-1541),  $MgO$  (ICDD Card No:01-075-1525) and  $LaOI$  (ICDD Card No: 01-073-2065) phases. The presence of  $MgO$  (*cubic*, *space group*= $Fm-3m$ ,  $a=b=c=4.198$  Å),  $LaOI$  (*tetragonal*, *space group*  $P4/nmm$ ,  $a=b=4.144$  Å,  $c=9.126$  Å),  $Mg_3(BO_3)_2$  (*orthorhombic*, *space group*= $Pnnm$ ,  $a=4.497$  Å,  $b=5.398$  Å,  $c=8.416$  Å) and  $LaB_6$  (*cubic*, *space group*= $Pm-3m$ ,  $a=b=c=4.157$  Å) phases were observed with all four reactions mixtures. Therefore, the magnesiothermic reduction reaction of  $La_2O_3$  in the presence of  $I_2$  does not follow as per the conventional understanding [21, 26, 27]. as stated in Equation 1, it rather follows as per the reaction given below in Eq 2. This mechanism is probably established for the first time for the synthesis  $LaB_6$  nanocrystals produced by magnesiothermic reduction process using  $I_2$ .

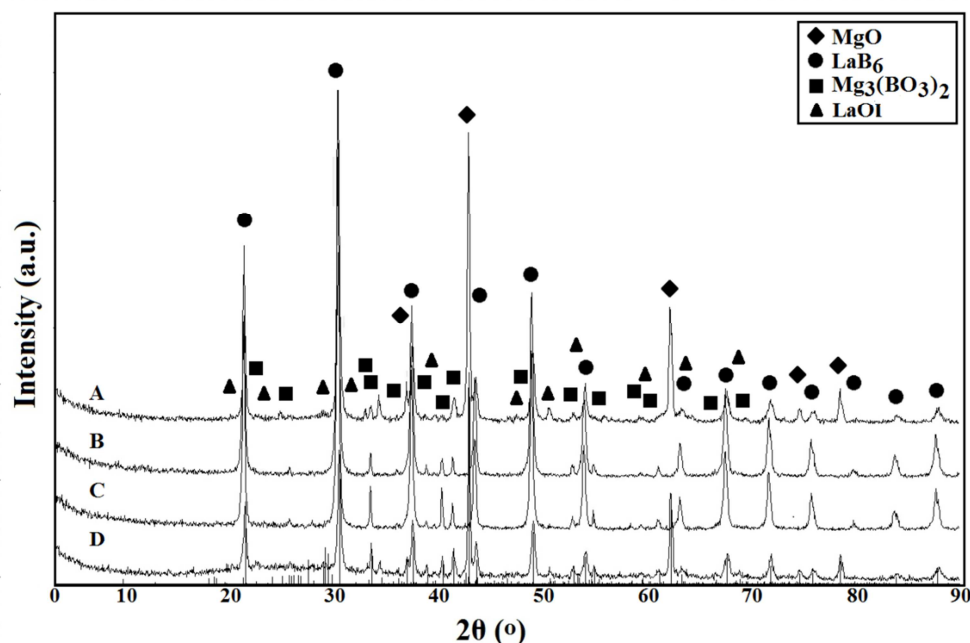
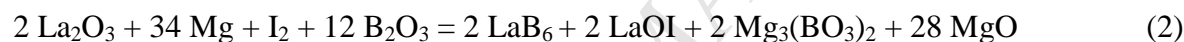
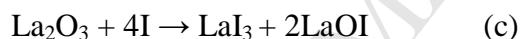
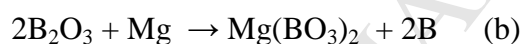


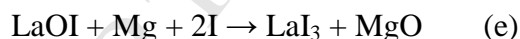
**Fig. 1.** XRD graphs of as-prepared powders obtained from the magnesiothermic reduction reactions using different molar ratios of the reactants,  $La_2O_3$ ,  $Mg$ ,  $I_2$ , and  $B_2O_3$ , (A: 1:44:6:12, B: 1:48:6.6:13.3, C: 1:58.5:8:16, D: 1:88:12:24, for starting powders of) XRD graph of powders obtained after explosive reactions with different molar ratios.



The standard Gibbs free energy ( $\Delta G$ ) and the standard enthalpy changes ( $\Delta H$ ) were determined using HSC Chemistry 6.0 software [28].  $\Delta G$  and  $\Delta H$  changes for the reaction of the powder mixture  $\text{La}_2\text{O}_3 + \text{B}_2\text{O}_3 + \text{Mg} + \text{I}_2$  to 2000 °C were calculated and plotted in Figure 2a. Figure 2a shows that the reaction of the starting powders at all temperatures between 0 to 2000 °C has a large negative Gibbs free energy and large enthalpy change. According to the estimation of the Gibbs free energy, the overall reaction of Eq. (2) is thermodynamically spontaneous ( $\Delta G = -5450 \text{ kJ mol}^{-1}$ ) and highly exothermic ( $\Delta H = -6350 \text{ kJ mol}^{-1}$ ) as reported elsewhere as well [26, 29]. Due to its high exothermicity, a massive internal heat is generated within the reacting species, and as an effect the internal temperature becomes much higher, which results in reduction of  $\text{B}_2\text{O}_3$  by Mg to B. All subsequent reaction steps for such reduction process for the formation of  $\text{LaB}_6$  are given below. It explains the role of  $\text{I}_2$  in this low temperature magnesiothermic reduction process for the synthesis of  $\text{LaB}_6$ , where  $\text{I}_2$  forms intermediate compounds with La that ultimately lead to form  $\text{LaB}_6$  releasing iodine back.



The probable reaction steps as shown above indicated that the higher concentration of Mg can induce the formation of more  $\text{LaI}_3$  by converting  $\text{LaOI}$  to  $\text{LaI}_3$  according to the eqn. (e), and consequently the formation of more  $\text{LaB}_6$ .



The XRD's also confirmed that mechanistically higher concentration of Mg can force the reaction to form more  $\text{LaB}_6$  and reduce the formation of  $\text{LaOI}$ , which also validates the proposed reaction pathway. As per the above reaction steps, a higher molar concentration of Mg must kinetically also favor the formation of  $\text{MgO}$  as shown in Eq.(e).

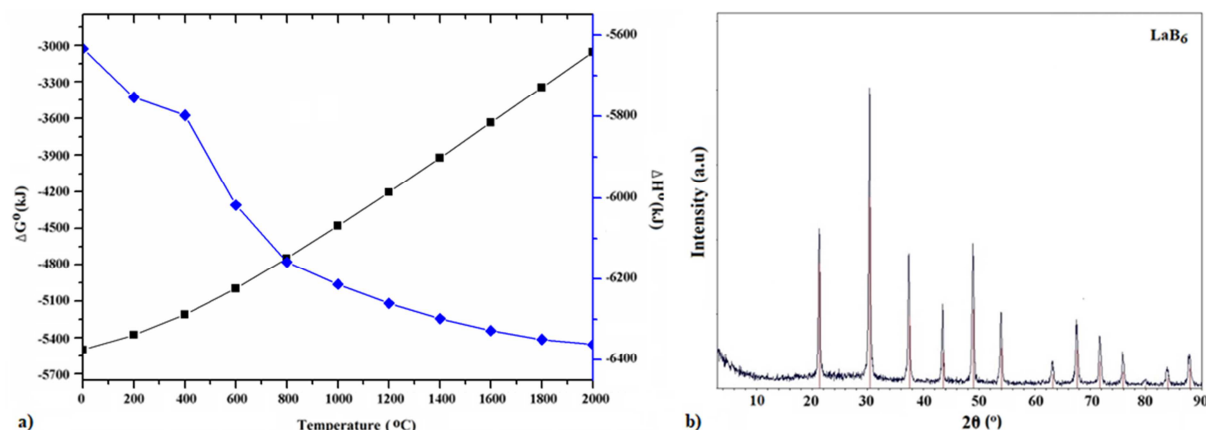


Figure 2. a) Gibbs free energy change (■) and enthalpy change (◆) versus temperature curves of the overall reaction in Eq.(2). b) XRD pattern of the  $\text{LaB}_6$  nanocrystals

After a thorough and careful washing with 5 M HCl solution, the  $\text{Mg}_3(\text{BO}_3)_2$ , LaOI and MgO phases were removed from the synthesized powders. After leaching the powder was further washed with deionized water. The thoroughly leached and washed powder was subjected to vacuum drying. The XRD pattern of the purified powder given in Figure 2b clearly showed that the final product of  $\text{LaB}_6$  was completely free from any undesirable contamination and the average crystallite size of  $\text{LaB}_6$  phase was determined as  $28 \pm 3.0$  nm by well-known Scherrer formula.

Figure 3 presents the Rietveld refinement applied to the XRD pattern of the purified sample. The grey (plus) and black lines shows the purified powders and calculated pattern of the modelled structure, respectively. The difference of the observed and calculated patterns is plotted in the lower part of the figure as a solid trace. The vertical bars refer to the calculated allowed Bragg reflections. Single phase Rietveld refinement confirms the structure of  $\text{LaB}_6$  in  $Pm-3m$  space group with the lattice parameters of  $a=b=c=4.153(2)$  Å. Table 2 presents the details of the basic crystallographic data for  $\text{LaB}_6$ . The diffraction peaks are well indexed and assigned to the parallel crystal plane of (100), (110), (111), (200), (210), (211), (220), (221), (310), (311), (222), (320) and (321). The obtained results are in good agreement with the previous data published in the literature [9, 24]. The diffraction data was *refined* on the *assumption* that the metal atoms would *occupy* the site 1a whereas non-metal *atoms* would be at the 6f site. The sharp and well-defined peaks in Fig. 3 indicated the high purity of the crystalline products. The average particle size was also determined as  $61.3 \pm 2.0$  nm by using the isotropic Lorentzian Scherrer particle broadening parameter (LX) of refined peak profiles.

Because of the polycrystalline nature of the synthesized  $\text{LaB}_6$  powder particles, the particulates are composed of many crystallites of varying sizes and orientations. Measuring crystallite sizes from XRD patterns is a well-known technic. SEM images revealed that individual crystallites within the relatively larger particle sizes.

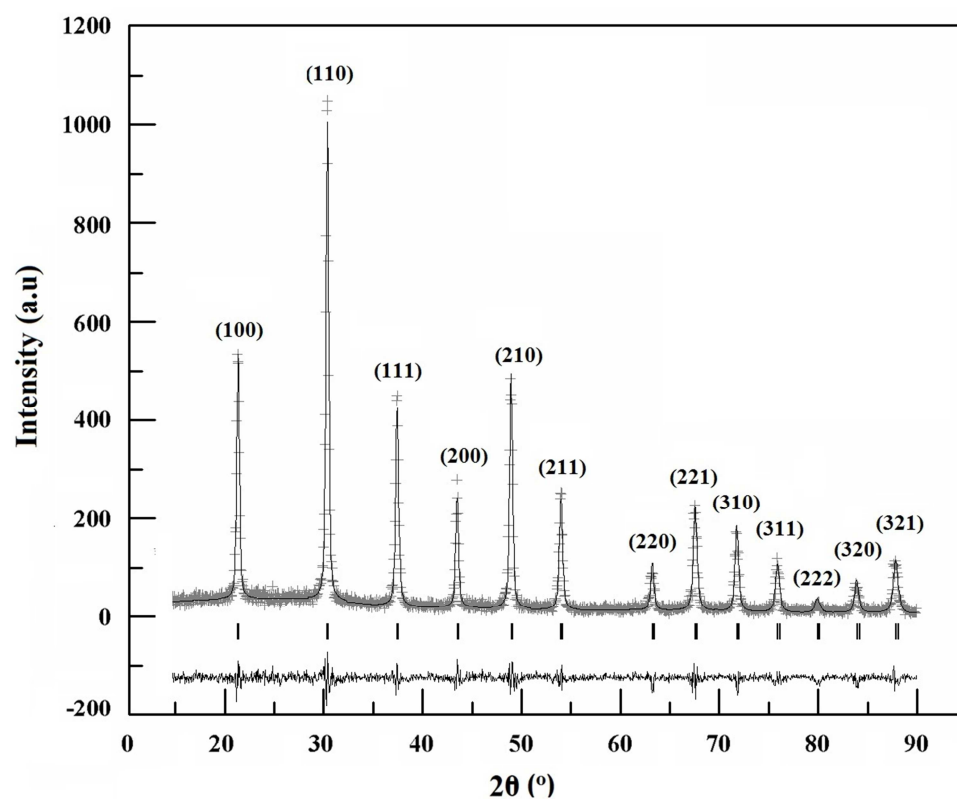
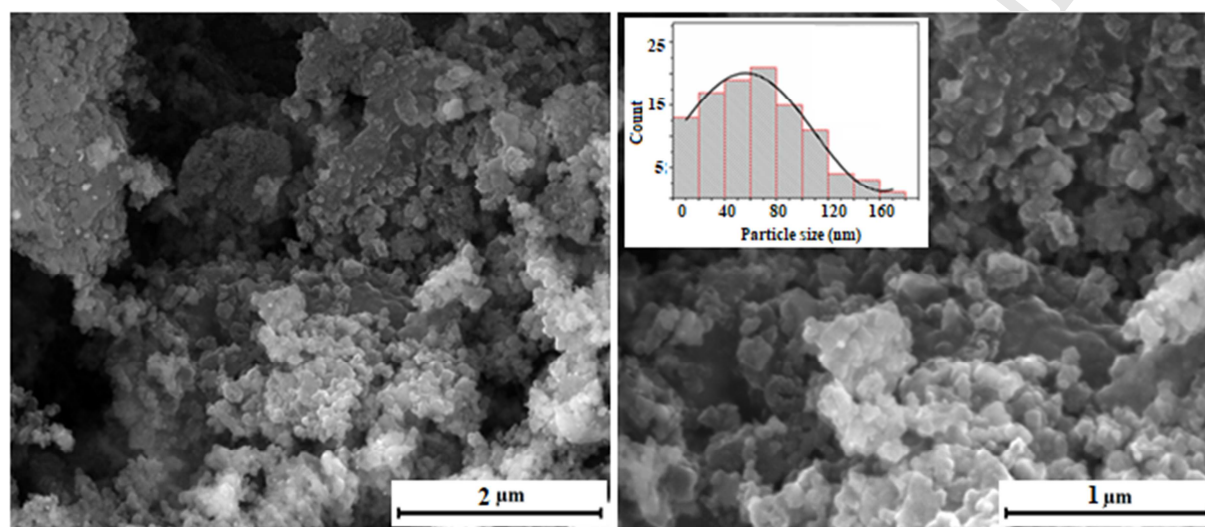


Figure 3. Rietveld refinement of  $\text{LaB}_6$ .

Table 2. Atomic positions and crystallographic data of  $\text{LaB}_6$

Formula	LaB <sub>6</sub>	Space group	<i>Pm-3m</i>		
Crystal system	<i>Cubic</i>	Data points	1739		
Unit cell dimensions (Å)	<i>a</i> = <i>b</i> = <i>c</i> = 4.154(3) <i>α</i> = <i>β</i> = <i>γ</i> = 90°	Unit cell volume (Å <sup>3</sup> )	71.7(4)		
2θ range refined	15-90°	R <sub>p</sub>	0.1329		
S (χ <sup>2</sup> )	1.421	R <sub>wp</sub>	0.1807		
Atomic positions					
Atom	site	x	y	z	Uiso
La	1 <i>a</i>	0	0	0	0.0016(2)
B	6 <i>f</i>	0.2018(4)	0.5	0.5	0.0027(3)

SEM images of the purified powders are shown in Fig.4. LaB<sub>6</sub> nano-particles thus produced were in clustered forms of many particles. An approximate size of those sample was estimated as  $78 \pm 12$  nm by ImageJ software. As expected, their agglomerations could have been due to the vacuum drying conditions during the purification steps. The similar observations were also reported elsewhere [26, 30]



**Fig 4.** SEM images of purified LaB<sub>6</sub> nanocrystals

The average particulate size of LaB<sub>6</sub> phase was determined as  $61.3 \pm 2.0$  nm and the specific surface area of the purified LaB<sub>6</sub> powder,  $1.3 \text{ m}^2/\text{g}$ , determined by BET method further signified that the nano-particulates are composed of many small LaB<sub>6</sub> units. The rationale of such approximation was realized from the structural information available on LaB<sub>6</sub> crystals. The crystal structure of LaB<sub>6</sub> is simple cubic (space group; Pm-3m), with Boron-octahedra in body-centered positions and La atoms at the corners of the unit cell. The crystal structure of LaB<sub>6</sub> comprising two unit-cells is shown in Fig. 5 as an illustration. As it can be seen boron atoms in each unit are in the form of octahedral cage. The bond length of B6-B7 in adjoining cells is the shortest in the LaB<sub>6</sub> crystal structure. The crystal structure studies by Hossain et al delineated that in LaB<sub>6</sub> there was a coexistence of covalent, ionic, and metallic bonds, which probably explains the reason for the high thermionic emissions of LaB<sub>6</sub> [25]. Going by its stoichiometry, a unit crystal of lanthanum hexaboride comprises 12 units of LaB<sub>6</sub> (La<sub>12</sub>B<sub>72</sub>; Mol. Wt. 2447.4) constituting  $2.5 \times 10^{20}$  such unit crystals per gram. From the measured surface area ( $1.3 \text{ m}^2/\text{g}$ ) and the average volume of each nano-particulate (considering spherical

sweeping volume for the nano-particles of  $\text{LaB}_6$  of size  $61.3 \pm 2.0$  nm for the sake of simplicity), the average mass of an individual particulate can be estimated in of the order of  $5 \times 10^{-15}$  g (considering the density of  $\text{LaB}_6$  as  $4.72 \times 10^6$  g/m<sup>3</sup>). From that estimated value it can be visualized that each particulate of an average size of  $61.3 \pm 2.0$  nm might comprise around  $10^5$  numbers of unit-crystals to constitute a nano-particulate. A similar value was also obtained from the surface area approximation of the nanoparticles and from the BET surface area value.

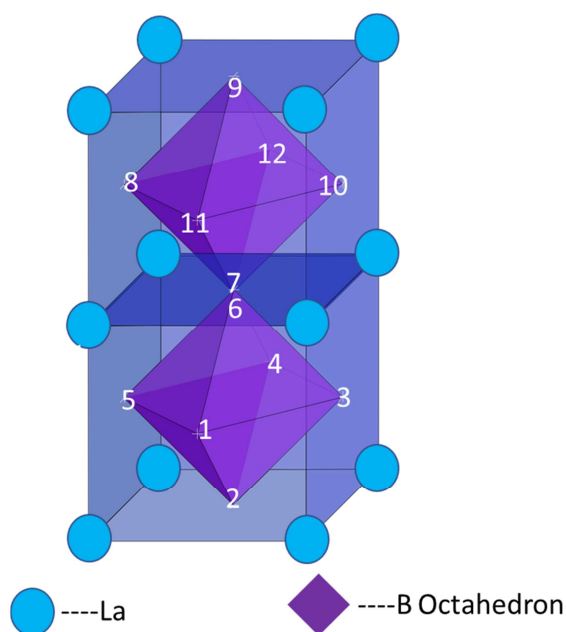


**Fig. 5.** In the crystal structure of Lanthanum hexaboride, two adjoining unit cells show the bonding between two adjacent octahedra of boron. The bond length of B6-B7 is the shortest distance in the structure.

#### 4. Conclusion

A viable method of synthesizing a very pure form of  $\text{LaB}_6$  nano-powders has been devised by adopting a low temperature synthetic route using  $\text{La}_2\text{O}_3$ ,  $\text{B}_2\text{O}_3$ , Mg and  $\text{I}_2$  under an inert atmosphere. The ball milling process increased the reactivity of the starting materials enabling the reaction to occur at temperatures around  $90^\circ\text{C}$ . Removal of all byproducts by leaching and washing helped forming nano- $\text{LaB}_6$  powders in very pure forms. The reaction mechanism for the formation of  $\text{LaB}_6$  was confirmed by XRD. From the specific surface area of the nano-powder ( $1.3\text{m}^2/\text{g}$ ) and from the average size of the nano-particulates ( $61.3 \pm 2.0$  nm), it

appears from the crystallographic approximations that each small nano-particulate is probably constituted roughly by  $10^5$  numbers of unit-crystals of  $\text{LaB}_6$  suggesting the fineness of the  $\text{LaB}_6$  nano-powder synthesized by the present technic.

### Acknowledgments

Authors would like to thank Etimaden Works General Managements, Head of Technology Development Department for using laboratory facilities and providing chemical materials.

### References

- [1] S. Reich, H. Suhr, K. Hanko, L. Szepes, Deposition of thin films of Zirconium and Hafnium Boride by plasma enhanced chemical vapor deposition, *Adv. Mater.* 4 (1992) 650-653.
- [2] H.E. Çamurlu, F. Maglia, Preparation of nano-size  $\text{ZrB}_2$  powder by self-propagating high-temperature synthesis, *J. Eur. Ceram. Soc.* 29 (2009) 1501-1506.
- [3] J.P. Kelly, K. Raghunath, O.A. Graeve, A Solvothermal Approach for the Preparation of Nanostructured Carbide and Boride Ultra-High Temperature Ceramics, *J. Am. Ceram. Soc.* 93 (2010) 3035-3038.
- [4] M. Barış, T. Şimşek, H. Gökmeşe, A. Akkurt, Characterisation of  $\text{W}_2\text{B}$  nanocrystals synthesized by mechanochemical method, *J. of Boron.* 1 (2016) 45-51.
- [5] Y. Hwang, J.K. Lee, Preparation of  $\text{TiB}_2$  powders by mechanical alloying, *Mater. Lett.* 54 (2002) 1-7.
- [6] H.Y. Qiu, W. M. Guo, J. Zou, G. J. Zhang,  $\text{ZrB}_2$  powders prepared by boro/carbothermal reduction of  $\text{ZrO}_2$ : The effects of carbon source and reaction atmosphere, *Powder Technol.* 217 (2012) 462-466.
- [7] M. Aksu, E. Aydın, Nano and micro-sized  $\text{EuB}_6$  via magnesiothermic reduction, *J Ceram Process Res.* 14 (2013) 4-7.

- [8] M. Zhang, X. Wang, X. Zhang, P. Wang, S. Xiong, L. Shi, Y. Qian, Direct low-temperature synthesis of RB<sub>6</sub> (R=Ce,Pr,Nd) nanocubes and nanoparticles, *J. Solid State Chem.* 182 (2009) 3098–3104
- [9] M. Zhang, L. Yuan, X. Wang, H. Fan, X. Wang, X. Wu, H. Wang, Y. Qian, A low-temperature route for the synthesis of nanocrystalline LaB<sub>6</sub>, *J. Solid State Chem.* 181 (2008) 294–297.
- [10] Y. Yuan, L. Zhang, L. Liang, K. He, R. Liu, G. Min, A solid-state reaction route to prepare LaB<sub>6</sub> nanocrystals in vacuum, *Ceram. Int.* 37 (2011) 2891–2896.
- [11] M. Kumari, S. Gautam, P. V. Shah, S. Pal, U. S. Ojha, A. Kumar, A. A. Naik, J. S. Rawat, P. K. Chaudhury, Harsh, R. P. Tandon, Improving the field emission of carbon nanotubes by lanthanum-hexaboride nano-particles decoration, *Appl. Phys. Lett.* 101 (2012) 123116-123122.
- [12] H.Y. Qiu, W.M. Guo, J. Zou, G. J. Zhang, Al-ZrB<sub>2</sub> powders prepared by boro/carbothermal reduction of ZrO<sub>2</sub>: The effects of carbon source and reaction atmosphere, *Powder Technol.* 217 (2012) 462–466.
- [13] L.Z. Pe, H.N. Xiao, B<sub>4</sub>C/TiB<sub>2</sub> composite powders prepared by carbothermal reduction method, *J Mater Process Tech.* 209 (2009) 2122–2127.
- [14] K. Bao, Y. Wen, M. Khangkhamano, S. Zhang, Low-temperature preparation of titanium diboride fine powder via magnesiothermic reduction in molten salt, *J Am Ceram Soc.* 100 (2017) 2266–2272.
- [15] S. Angappan, N. Kalaiselvi, R. Sudha, A. Visuvasam, Electrochemical Synthesis of Magnesium Hexaboride by Molten Salt Technique, *Int. Sch. Res Notices.* 2014 (2014) 1-6.
- [16] M. Baris, T. Şimşek, H. Taşkaya, A. K. Chattopadhyay, Synthesis of Fe-Fe<sub>2</sub>B Catalysts via Solvothermal Route for Hydrogen Generation By Hydrolysis Of NaBH<sub>4</sub>, *J. of Boron.* 3 (2018) 51 – 62.



- [17] C.L. Yeh, H.J. Wang, Preparation of borides in Nb–B and Cr–B systems by combustion synthesis involving borothermic reduction of Nb<sub>2</sub>O<sub>5</sub> and Cr<sub>2</sub>O<sub>3</sub>, *J. Alloys and Compd.* 490 (2010) 366–371.
- [18] J.Abenojar, F.Velasco, J.M.Mota, M.A.Martinez, Preparation of Fe/B powders by mechanical alloying, *J. Solid State Chem.* 177 (2004) 382–388.
- [19] S. Otani, S. Honma, Y. Yajima, Y. Ishizawa, Preparation of LaB<sub>6</sub> single crystals from a boron-rich molten zone by the floating zone method, *J. Cryst. Growth.* 126 (1993) 466–470.
- [20] W. Rasband, ImageJ, Image Processing and Analysis in Java, National Institutes of Health, USA, 1.50V, (2014).
- [21] A.C. Larson, R.B.V. Dreele, GSAS: General structure analysis system report LAUR 86-748. Tech. Rep., Los Alamos National Laboratory (2000).
- [22] M. Baris, T. Simsek, T. Simsek, S. Ozcan, B. Kalkan, High purity synthesis of ZrB<sub>2</sub> by a combined ball milling and carbothermal method: Structural and magnetic properties, *Adv. Powder Technol.* 29 (2018) 2440–2446.
- [23] W. Han, Z. Wang, Q. Li, H. Liu, Q. Fan, Y. Dong, Q. Kuang, Y. Zhao, Autoclave growth, magnetic, and optical properties of GdB<sub>6</sub> nanowires, *J. Solid State Chem.* 256 (2017) 53–59.
- [24] L. Wang, L. Xu, Z. Ju, Y. Qian, A versatile route for the convenient synthesis of rare-earth and alkaline-earth hexaborides at mild temperatures, *Cryst. Eng. Comm.* 12 (2010) 3923–3928.
- [25] K. Bao, C. Liu, B. Yazdani Damavandi, S. Zhang, Low-Temperature Preparation of Lanthanum Hexaboride Fine Powder via Magnesiothermic Reduction in Molten Salt, *J. Ceram. Sci. Tech.* 07 (2016) 403–408.
- [26] D. Agaogullari, I. Duman, M. L. Ovecoglu, Synthesis of LaB<sub>6</sub> powders from La<sub>2</sub>O<sub>3</sub>, B<sub>2</sub>O<sub>3</sub> and Mg blends via a mechanochemical route, *Ceram. Int.* 38 (2012) 6203–6214.



- [27] B. Lihong, W. Wei, O. Tegus, A new route for the synthesis of submicron-sized  $\text{LaB}_6$ , Mater. Charact. 97 (2014) 69-73.
- [28] HSC Chemistry 6.0, Chemical Reaction and Equilibrium Software with extensive thermochemical database, Outokumpu. 2006.
- [29] J. A. Dean, in Lange's Handbook of Chemistry, McGraw-Hill, New York, 13th edn, 1985, Section 6; I. Barin, G. Platzki, in Thermochemical Data of Pure Substances, Wiley-VCH, Weinheim, 1995.
- [30] M. Hasan, H. Sugo, E. Kisi, Low temperature carbothermal and boron carbide reduction synthesis of  $\text{LaB}_6$ , J. Alloys and Compd. 578 (2013) 176–182
- [31] F. M. Hossain, D. P. Riley, G. E. Murch, Ab initio calculations of the electronic structure and bonding characteristics of  $\text{LaB}_6$ , Phys. Rev. B 72 (2005) 235101-235106.

**Highlights**

- Low temperature synthesis of pure  $\text{LaB}_6$  via magnesiothermic method.
- Rietveld refinements of  $\text{LaB}_6$  and its structural properties.
- Each particle seemed to be constituted by  $10^5$  numbers of unit crystal cells.
- Purification of unwanted phases by aqueous acid solution.